

Sediment transport trend in an erosive sandy beach: the case of Matinhos Beach, south coast of Brazil

David M. Luersen¹, Alexandre B. Lopes², Guilherme. A. S. Franz²,
Danilo Mildemberger³, Mauricio A. Noernberg^{2*}

¹ Pós-Graduação em Sistemas Costeiros e Oceânicos – Universidade Federal do Paraná (C.P. 61, 83255-976 – Pontal do Paraná – PR – Brazil).

² Centro de Estudos do Mar – Universidade Federal do Paraná (C.P. 61, 83255-976 – Pontal do Paraná – PR – Brazil).

³ Sistema de Tecnologia e Monitoramento Ambiental do Paraná – Centro Politécnico – Universidade Federal do Paraná (C.P. 19100 – 81531-980 – Curitiba – PR – Brazil).

* Corresponding author: m.noernberg@ufpr.br

ABSTRACT

Sandy beaches have different shoreline change rates (i.e., erosion/accretion rates). An erosive process on beaches poses risks for human-occupied areas. One example is Matinhos Beach (state of Paraná - Brazil), which has an average annual erosion rate of around 1.5 m yr⁻¹. This study applied a methodology that combines in situ measurements and numerical modeling to simulate the physical processes in the coastal area of Matinhos during the 2018 Austral winter. Monthly DGPS surveys were carried out in the study area from June to September. The MOHID modeling system was applied to simulate hydrodynamics and sediment transport, considering waves and tidal forcing validated with in situ data. The WAVEWATCH III and SWAN models were applied in a nesting approach to simulate the waves at Matinhos Beach. The GFS was used to assess the wind conditions. The study period showed a dynamic evolution of accretion and erosion between monthly measurements with no clear pattern in most profiles. Significant sand accumulation was observed near the headland. Morphological changes were minor due to the predominance of low energy without significant storm events. The measured morphological changes are in line with the residual littoral drift obtained from the modeling results for the period. The residual current velocities were towards the southwest, with magnitudes ranging from 0.15 m s⁻¹ to 0.2 m s⁻¹. A slight variation in the angle of wave incidence (10°) may change the direction (southwest or northeast) and intensity of the littoral drift. The applied methodology can reduce uncertainty and support effective coastal management. However, the seasonal scales of wave climate cannot be disregarded, nor can the need for coastal oceanographic data.

Keywords: Coastal processes, Numerical modeling, MOHID, Coastal management, Sediment transport

INTRODUCTION

Coastal areas with sandy beaches are highly populated and occupied because of their aesthetic benefits and amenities, and they receive millions

of visitors for recreational activities such as swimming, surfing, and camping (Marzetti et al., 2016; Luijendijk et al., 2018). From an economic point of view, coastal areas are public goods, and their preservation is an essential task of public authorities, but public funds are limited (Houston, 2013; Marzetti et al., 2016).

Sandy shorelines are more susceptible to changes and account for 31% of the world's ice-free shorelines. Approximately 24 % of sandy beaches

Submitted: 20-Jun-2023

Approved: 08-Jan-2024

Associate Editor: Eduardo Siegle



© 2024 The authors. This is an open access article distributed under the terms of the Creative Commons license.

worldwide are experiencing erosion rates surpassing 0.5 m yr^{-1} . In contrast, 28% of the beaches accumulate sand, while nearly 48% remain stable. However, in human-occupied areas, erosion becomes a coastal risk (Griggs, 2005) with three main characteristics: loss of areas with economic value, destruction of natural defense systems, and weakening of artificial coastal defenses (Alexandrakis et al., 2015). The first assessment of the global effects of climate-induced sea level rise on sandy beach erosion estimated a global land loss of about 6,000–17,000 km^2 during the 21st century, leading to 1.6–5.3 million people being forced to migrate (Hinkel et al., 2013). The 21st century will significantly increase coastal risks, projected to surge by at least tenfold. This surge is attributed to the unavoidable rise in sea levels, which will profoundly affect ecosystems, human populations, livelihoods, infrastructure, food security, cultural and natural heritage, and efforts for climate mitigation along the coast. These characteristics highlight the need for interventions that minimize the effects of coastal erosion.

In coastal regions, the diversity of actors with different or opposing interests causes significant social pressure (Cooper and Mckenna, 2008). Moreover, these regions are complex systems with various physical processes controlling their dynamics, which makes management and decision-making difficult (Billé, 2008). Therefore,

understanding local coastal processes is a prerequisite for achieving sustainable development along the coast, minimizing the potential risks posed by inefficient or flawed interventions.

The city of Matinhos, on the South coast of Brazil (Figure 1), is a popular tourist destination known for its sandy beaches, attracting thousands of visitors throughout the year, especially during the summer (Angelotti and Noernberg, 2010). The city has experienced intense urban growth since the 1950s, when there were no proper occupation regulations, which resulted in the construction of roads and houses on the upper part of the beach (Sampaio, 2006). Its resident population rose from 4,000 in 1970 to 40,000 in 2022. The city experienced notable consequences stemming from the destruction of foredune ridges and increased urbanization in the beach's dynamic zone. These factors contributed to coastal erosion issues across multiple sectors (Angulo et al., 2018). In addition, to protect the coast, a stone seawall was built, which, together with previous constructions, led to a significant change in the natural beach dynamics, triggering erosion processes that still exist today. The average annual erosion rate from 2001 to 2014 was 1.5 m yr^{-1} near the mouth of the Matinhos River (Bessa Jr., 2003; Angulo et al., 2016; Novak et al., 2016; Angulo et al., 2018).

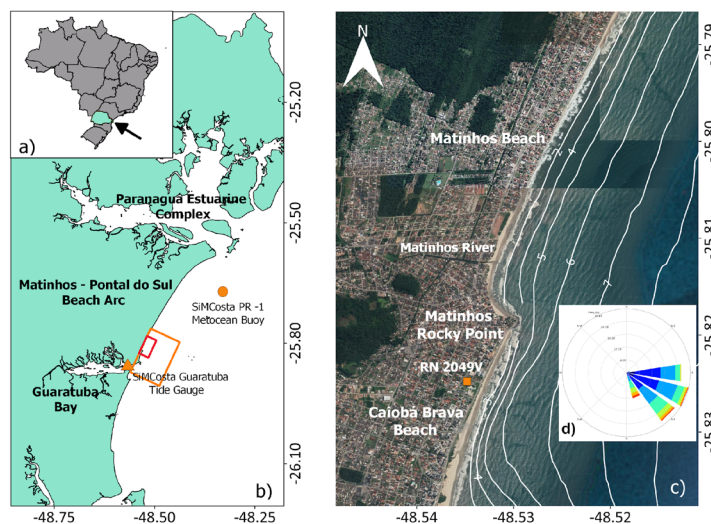


Figure 1. Location of the study area. (a) Location of the state of Paraná (in green) in Brazil. (b) Coastline of the state of Paraná with the location of the study area (the red rectangle is the model domain 1 and the orange rectangle is the model domain 2). (c) Satellite image (Landsat 8 / Copernicus, 2018) of the study area (red rectangle in b) with bathymetric depth contours (in white). (d) Jan/2014 to Jul/2015 wave rose obtained by SiMCosta PR-1 meteocean buoy.

The effects of erosion on the city's infrastructure have already led to the development of proposals for coastal management plans to avoid related problems (Angulo et al., 2016; Paraná State Government, 2019). In 2022, hard structures (groins and jetties) were constructed, and sand nourishment was performed on Matinhos Beach to mitigate erosion problems, with an approximate sand supply of 3 million cubic meters (Ratton, 2020). This study was carried out before this intervention and can be used as a reference in future studies to assess changes in the coastal system dynamics.

The process of beach erosion—straightness and lowering—present on Matinhos beach and the constant problems caused by coastal erosion are the motivation for improving the understanding of local coastal processes. In this work, the morphological changes on the beach were identified and linked to hydrodynamics and coastal sediment transport. During the austral winter period of 2018, measurements of beach topography, bathymetry, and sediment granulometry were obtained to identify beach changes and create numerical models to simulate waves, hydrodynamics, and sediment transport in the area. The morphological changes investigated in situ were compared with the transport trends obtained via numerical modeling.

METHODS

STUDY AREA

The Matinhos – Pontal do Sul Beach Arc is approximately 34.5 km long and is located in the central part of the coast of the state of Paraná, between the Guaratuba Bay and Paranaguá Estuarine Complex, South coast of Brazil. The study area is located in the southernmost region of the Beach Arc (Figure 1), in the municipality of Matinhos (25°49'8"S e 48°32'29"W). Its alongshore and cross-shore extensions are 6 km and 3 km, respectively, and extend to a depth of 10 m. Its southern limit is the headland Matinhos Rocky Point ("Pico de Matinhos" in Portuguese), the division between the Caiobá Brava Beach to the south and Matinhos Beach to the north. The beach near the headland has a typical log-spiral form, The beach adjacent to the headland exhibits a characteristic log-spiral shape, but human presence has disrupted the natural

shoreline configuration, resulting in persistent beach erosion issues. Towards the north, the beach has a rectilinear shape and relatively simple dynamics (Angulo, 2000).

The Paraná coastline experiences a semidiurnal tide pattern characterized by diurnal variances and nonlinear co-oscillation interactions. At the mouth of the Paranaguá Estuarine Complex, the spring tide range is 1.75 m. During the neap cycle, up to six high and low tides with a range of 0.3 m are formed (Lana et al., 2000). The wave climate mainly influences the beach. According to data collected by the SiMCosta PR-1 metocean buoy moored at a depth of 17 m, the mean significant wave height (H_s) was 1.01 m, with a maximum significant wave height of 2.3 m and a mean peak period (T_p) of 6 s, from January 2015 to June 2015. According to the World Meteorological Organization classification, the waves that reach the coast are predominantly light, with around 88% of H_s recorded below 1.25 m. The waves measured by the buoy were predominantly generated by local effects (87%), with only 13% showing $T > 8.0$ s. During the austral winter, 26% of the waves were moderate ($H_s > 1.25$ m), while in the summer, only 14% were moderate. The waves were predominantly from the ESE (29.98%) and SE (29.40%) (Figure 1d), but those with the greatest heights were from the SSE ($H_s = 1.35$ m), probably associated with more frequent frontal systems in winter (Oliveira et al., 2019). The combination of south-southeast winds, a rise in sea levels (storm surge), and large waves represents the highest energy events on the coast, intensifying coastal currents (Noernberg and Alberti, 2014). Water levels can rise up to 80 cm above the astronomical spring high tide during storm surges (Marone and Camargo, 1994).

The Matinhos – Pontal do Sul Beach Arc primarily comprises well-developed, polycyclic fine quartz sand sourced from the continental shelf and carried ashore by waves and currents (Souza et al., 2012). The grain size increases towards the south, transitioning to an intermediate-state rhythmic bar (Borzone et al. 1996; Angulo et al., 2016). There is sediments are interchanged between the exposed and submerged sections of the beach, and, during the summer, the subaerial beach sand volume increases (Angulo et al., 2016). The movement of sediment along the coast is primarily influenced by waves, particularly

favoring northward currents, at a rate of 104 - 105 $\text{m}^3 \text{yr}^{-1}$ (Sayão, 1989; Angulo et al., 2016).

DGPS MEASUREMENTS

The methodology applied for the DGPS topographic and bathymetric geodetic measurements was made using Post-Processed Kinematic (PPK) surveys with three GNSS Leica Viva GS15 receivers, following a methodology first applied by Ferreira et al. (2014). The first receiver was set as a base station at reference level (RN) IBGE 2049V with known coordinates at the SESC Caiobá Hotel (Figure 1) in Matinhos and at a normal altitude of 4.3587 m. The other two receivers acted as rovers for the beach topographic data survey. For the bathymetric data survey, a Garmin echoMAP CHIRP 42dv sonar was used together with a GNSS receiver acting as a rover, and both data groups were synchronized using its obtaining time. Post-processing procedures were carried out using Leica Geo Office Software. Geodetic measurements were obtained in GRS80 ellipsoidal height and converted into orthometric height using the MAPGEO 2010 geoid model (IBGE, 2018) afterward.

Topographic geodetic measurements were made with an epoch period of 1s, which resulted in approximately 21,000 points per survey. The surveys were carried out at spring tides, with low tide being the central time for broader beach coverage. The average survey time was approximately 4 hours. The potential maximum height error for the collected data is about 10 cm, mainly due to inaccuracies of the topographic surveying method with human walking.

Nearshore bathymetric data (10 m depth) were collected in April 2018 to improve nautical chart data, while beach topographic data were collected monthly from June to October 2018. In this type of survey, there is no need for tidal correction because the depth measured by the echo sounder is linked to the same reference level (ellipsoid of revolution - GRS80). That is, the geometric altitude of the bottom is equivalent to the geometric altitude of the transducer obtained by GNSS subtracted from the bathymetric data. In this way, topographic and bathymetric surveys are in the same vertical reference.

NUMERICAL MODELING

The MOHID Water Modeling System (Leitão et al., 2008; MARETEC, 2017) was coupled to

the third-generation wave model SWAN (Booij et al., 1999) to assess hydrodynamics and sediment transport in the study area, following a methodology previously described by Franz et al. (2017a).

MOHID is a three-dimensional water modeling system that integrates different modules (e.g. hydrodynamics, water properties, water quality, sediment) that make it possible to simulate hydrodynamic fluxes, the transport of water properties and sediment, ecological processes, and water quality parameters. MOHID uses the finite volume method for spatial discretization. Its code is written in the ANSI FORTRAN 95 language and is available in the GitHub repository.

The hydrodynamic module computes the three-dimensional (3D) or two-dimensional depth-averaged (2DH) velocity field and surface elevation using the continuity and momentum primitive equations, assuming the hydrostatic, Boussinesq, and Reynolds approximations (Martins, 2000; Leitão, 2003). The vertical turbulent viscosity was computed using the GOTM turbulence model (Umlauf et al., 2018). The intertidal zones were represented by a wetting/drying scheme (Martins et al., 2001), considering where the cells were uncovered below, with null mass and momentum fluxes.

Non-cohesive sediment transport is divided into bedload and suspended sediment transport (Franz et al., 2017b). Suspended sediment transport was calculated by solving the advection/diffusion equations. Bedload was solved following the semi-empirical formulation of Soulsby and Damgaard (2005), considering the effect of waves and currents (Franz et al., 2017a).

NUMERICAL MODEL SETUP

The simulation domain was divided into two subdomains. The first domain (Level 1), represented by the orange rectangle in Figure 1, covers the area from the mouth of Guaratuba Bay to beyond the northern boundary of the study area, providing boundary conditions for the second domain (Level 2), which is represented by the red rectangle in Figure 1. The water level boundary conditions, current velocity components (u and v), and wave parameters in Level 2 were obtained from Level 1. This one-way offline nesting was used to avoid creating shadow zones in the higher

resolution domain (Level 2) and to consider the wave energy dissipation caused by the Guaratuba Bay ebb-tidal delta, mainly due to waves coming from the south.

Level 1 has 250 rectangular grid cells with a uniform spatial resolution of 50 m along the shore and a variable spatial resolution between shores, ranging from 10 m on the nearshore to 100 m offshore. Boundary conditions for the Level 1 water level were obtained by a previous application of the MOHID model on the Paraná coast as part of the “Sea Observatory and operational modeling system for the south-eastern Brazilian shelf” (Franz et al., 2021), which includes the effects of the astronomical tide and storm surges. Boundary conditions for wave parameters (significant height, direction, length, mean period, bottom orbital velocity, and radiation stress) were obtained using the SWAN wave model for the Paraná coast, implemented in the scope of this study (see next section).

Level 2 has a higher resolution to represent the hydrodynamics and sediment transport processes in the surf zone up to the subaerial beach. This simulation domain has 236 grid cells with a uniform spatial resolution of 20 m alongshore and a variable grid cell resolution between shores, ranging from 5 m on the nearshore and subaerial beach to 45 m offshore.

Hydrodynamics and sediment transport were simulated for the period from 2018/06/12 to 2018/09/30 without considering morphological changes. The simulations were carried out following a two-dimensional depth-averaged (2DH) approach. The roughness length (z_0) was set uniformly to 2.5 mm, and the horizontal viscosity was set to $0.5 \text{ m}^2 \text{ s}^{-1}$.

The water level data used in the model were validated with the available data measured by the Guaratuba Bay SiMCosta tidal gauge for the period from 2018/07/12 to 2018/08/11 (Figure 2). The morphological changes investigated in situ were compared with the transport trends obtained via numerical modeling.

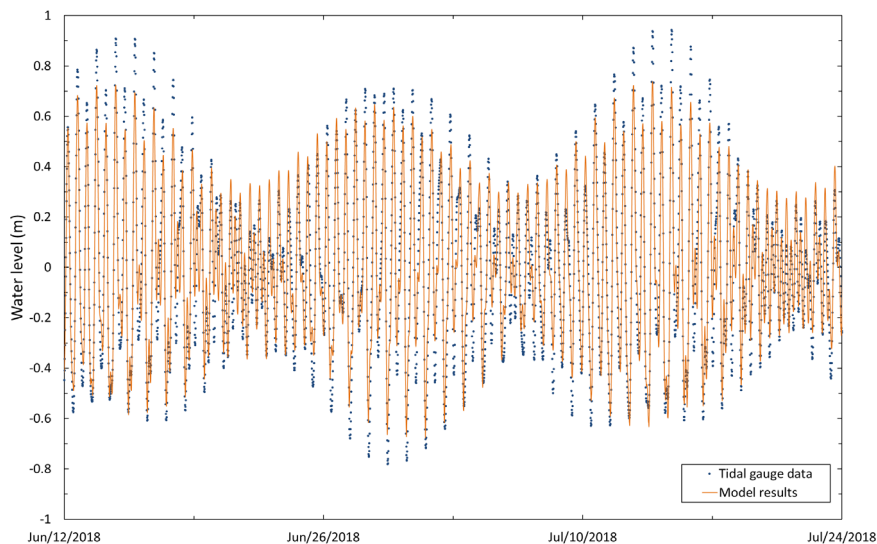


Figure 2 . Modeled results and water level measured by the Guaratuba Bay SiMCosta tidal gauge.

WAVE PARAMETERS

Two wave models were implemented to obtain wave parameters (significant wave height, mean period, mean direction, and orbital velocities). The WAVEWATCH III (WWIII) (Tolman et al., 2002; Tolman, 2009) wave model was implemented using a nesting technique and forced by wind results obtained from the Global Forecast System – GFS (NOAA, 2018). The WWIII

model provided the boundary conditions for the SWAN model, representing the coast of Paraná with better resolution.

The WWIII simulation was carried out using three domains in a nesting approach, in which the first domain encompasses the South Atlantic Ocean with a spatial resolution of 0.5° , the intermediate domain represents the Brazilian coast with a resolution of 0.125° , and the last domain represents

the southwestern part of the Brazilian continental shelf with a spatial resolution of 0.025°. The Paraná coast SWAN model has a spatial resolution of 500 m. The MOHID domains level 1 and 2 have a SWAN wave model coupled to them with the same dimensions and grid resolutions.

The wave results from the WWIII and SWAN models used to force the hydrodynamics and sediment transport simulations were validated using the data recorded by the SiMCosta PR - 1 metocean buoy for the period from January to May 2015 (Figure 1d). The wave parameters compared were significant height (H_s), mean direction (D_m), and mean period (T_m). The performance of the modeled wave and water level results was evaluated using the Pearson Correlation Coefficient, Root Mean Square Error (RMSE), and Bias.

SEDIMENT PARAMETERS

Sediment samples were collected from the upper, medium, and lower parts of the beach in four different profiles, shown as profiles II, III, IV, and V in Figure 3, and analyzed using a MICROTAC Bluewave laser granulometer. These samples provided the median sediment grain size (D_{50}) values for the subaerial beach. The D_{50} values for the submerged parts of the study area were obtained from the samples collected by Veiga (2004).

Due to the low number of profiles in the sediment collected, a modeling technique was used to better visualize the sediment distribution in the study area, considering the D_{50} values obtained from the surveys as the initial condition (Franz et al., 2017b). Following this approach, the model (Level 2) was spin-up for seven days with a morphological acceleration factor (MORFAC) 365.

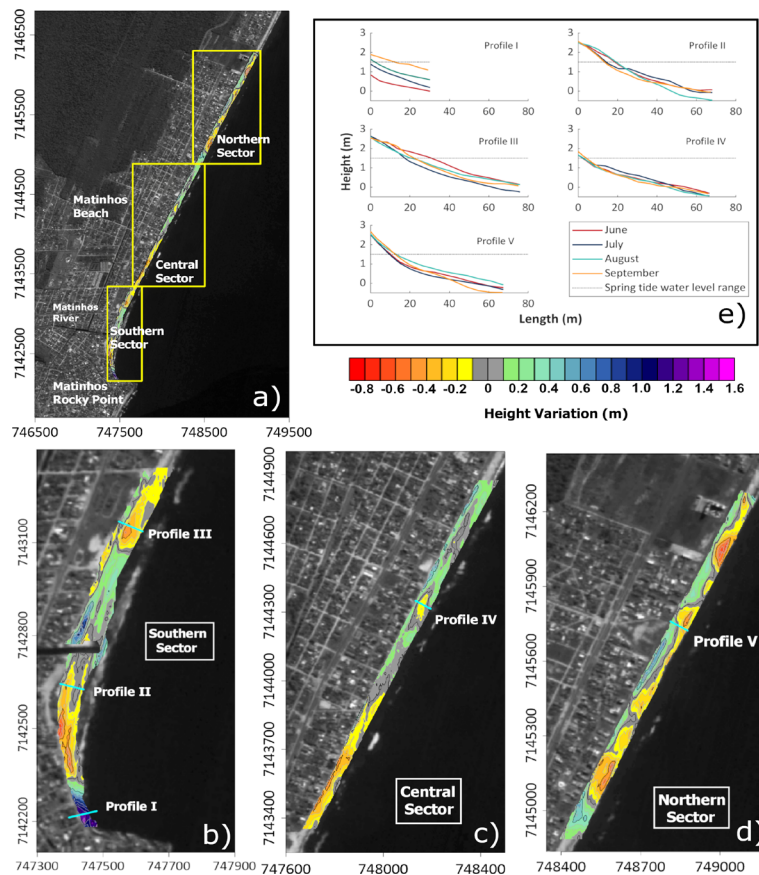


Figure 3. Morphological changes at Matinhos Beach obtained via DGPS topographic survey during the study period. The color bar represents the morphological changes in height for subfigures (a), (b), (c), and (d), where cool colors (blue) represent positive variations (accretion) and warm colors (red) represent negative variations (erosion). The gray color represents the potential error associated with the data collection method. A) Location of the sectors within the study area. B) Southern Sector. C) Central Sector. D) Northern Sector. E) Cross-view of the monthly changes for Profiles I, II, III, IV, and V, with the mean spring tide high water range shown by the black dotted line.

The sediment in the area was classified as fine and medium sand, with D50 values ranging from 0.18 mm to 0.3 mm. The highest D50 values in the

area were near the wave breaking zone and had a decreasing gradient in the direction of the sea and the beach. Figure 4 shows the initial conditions for D50.

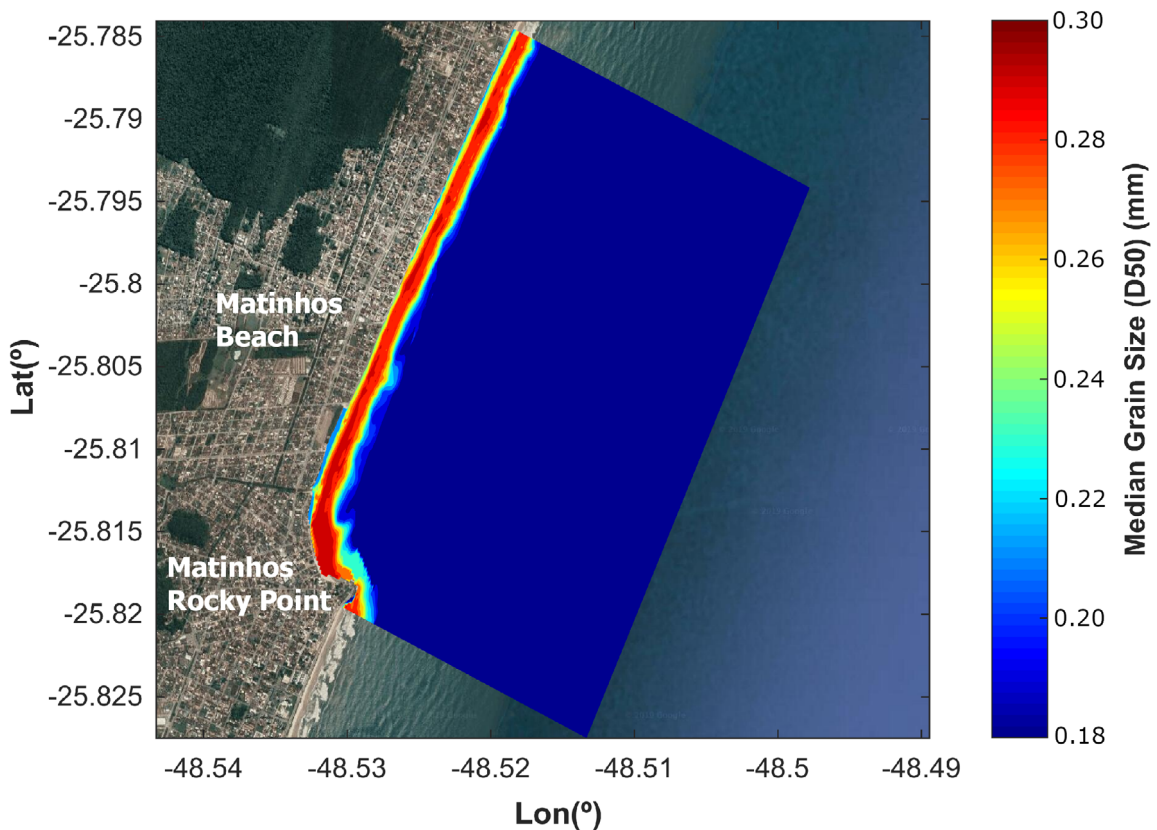


Figure 4. Median grain size (D50) of the sediments distributed within the study area, obtained via numerical simulation according to the local hydrodynamics.

RESULTS

Figure 3a-d shows the in situ data of the beach profiles (sectional view) chosen to show the morphological changes on the subaerial beach, along with the Digital Elevation Model representing the total height difference of the beach morphology from June to September 2018.

The profiles numbered II, III, IV, and V were chosen according to the sediment collection described above, and Profile I was chosen because it represents a zone of interest close to the headland. The offshore depth limit of the profiles was defined based on the survey with the lowest number of topographic points in the

offshore direction, which justifies the short length of Profile I throughout the whole period. The upper beach limit was defined based on non-dynamic physical barriers (e.g. rocks, dense vegetation, and seawall) (Figure 3e).

Profile I is located next to the headland, limiting the study area to the south. In this region, the upper beach is bounded by rocks that act as natural barriers to the incidence of waves from the southeast. It can be seen that, in the first months of the survey, the entire beach profile was submerged during the high spring tide, which changed as accretion occurred during the following months.

Further north of the headland and close to the Matinhos River (Figure 3b) is Profile II, in a region where local fishermen dock their boats. In this area, not many significant features block sediment movement, as it is located in the wave incidence shadow zone created by the headland. Profile III is located in the region within the study area that contains the most natural morphological features, including some small dunes in the upper beach (not present in the profile). It is an area that was recovered thanks to the removal of some irregular properties by the local authorities in the early 2000s (Angulo et al., 2016).

In contrast to Profile III, the most altered and urbanized area of the study area is represented by Profile IV, in a region where the coastal road was built over the upper beach and later a seawall was built to protect it and nearby properties (Angulo et al., 2016). Profile IV shows the deepening of the beach to sea level compared with the other profiles. It is also possible to observe, in general, the shortening of the beach face, which is almost nonexistent during the high spring tide.

The northern limit of the study area is represented by Profile V and, despite the existence of the seaside road, has more natural characteristics than the region where Profile IV is located. This status might be attributed to the absence of a seawall and the greater distance from the beach to the road.

The backshore composition controls the feature of the profiles. Small sand reservoirs on the backshore give the profile a gentler slope and a larger beach face (Profiles II and III). The absence of these reservoirs (rocks, seawall, roads) shortens the beach and increases its slope (Profiles I, IV, and V). Although these morphological changes are subtle, they are evident even considering the small relative distance between the profiles (hundreds of meters).

Morphological changes were minor during the Austral winter of 2018 due to the predominance of light waves without significant storm events. This inference is based on the team's field observations, the monitoring of oceanographic conditions during the period, and the wave model output, as there are no in situ measurements of the sea state in the region.

The study period showed a dynamic evolution of accretion and erosion between measurements, with no clear pattern in most profiles. However, a cyclical erosion/accretion pattern was observed alongshore, with vertical variations of less than 1 meter (Figure 3a). The southern part (Profile I) stood out from the rest of the area for having a clear accretion pattern during the survey, with a vertical variation of approximately 1 m.

WATER LEVEL AND WAVES

Table 1 shows the statistical performance of the SWAN and MOHID models for wave and water level parameters. The amplitude and phase results are generally very accurate for the water level data, with the modeled data slightly overestimating the amplitude (up to 0.22 m) (Figure 2). Thus, the coastal model is suitable for providing boundary conditions for local applications, as done in this study.

Table 1. Performance of SWAN and MOHID for wave and water level parameters used in the hydrodynamics and sediment transport simulations. Hs is the significant height; Tm is the mean period; and Dm is the mean direction.

Statistics	Hs	Tm	Dm	Water Level
Pearson Correlation	0.81	0.67	0.73	0.95
RMSE	0.21	1.12	18.01	0.11
Bias	-0.02	1.30	-9.48	0

The model also slightly underestimated the wave peaks (up to 0.67 m) and overestimated the wave periods (up to 4.05 s), despite the good statistical performance (Figure 5). The performance of each wave parameter can be assessed in the scatterplots in Figure 6.

The statistical results for the modeled wave parameters found in this study (Table 1) are similar to other wave modeling studies carried out in southern Brazil (Oliveira et al., 2019; Cecilio and Dillenburg, 2020). Figure 7 shows the modeled

results for significant wave height and mean wave direction in the breaker zone in the center of the study area (next to Profile IV, shown in Figure 3c). The results showed an average wave height of 0.88 m and only one event in which

the wave height approached 2 m in the study area. Mean wave directions ranged from east to southeast, the predominant wave directions in the region. The mean wave periods ranged from 4 to 8 s during almost the entire period.

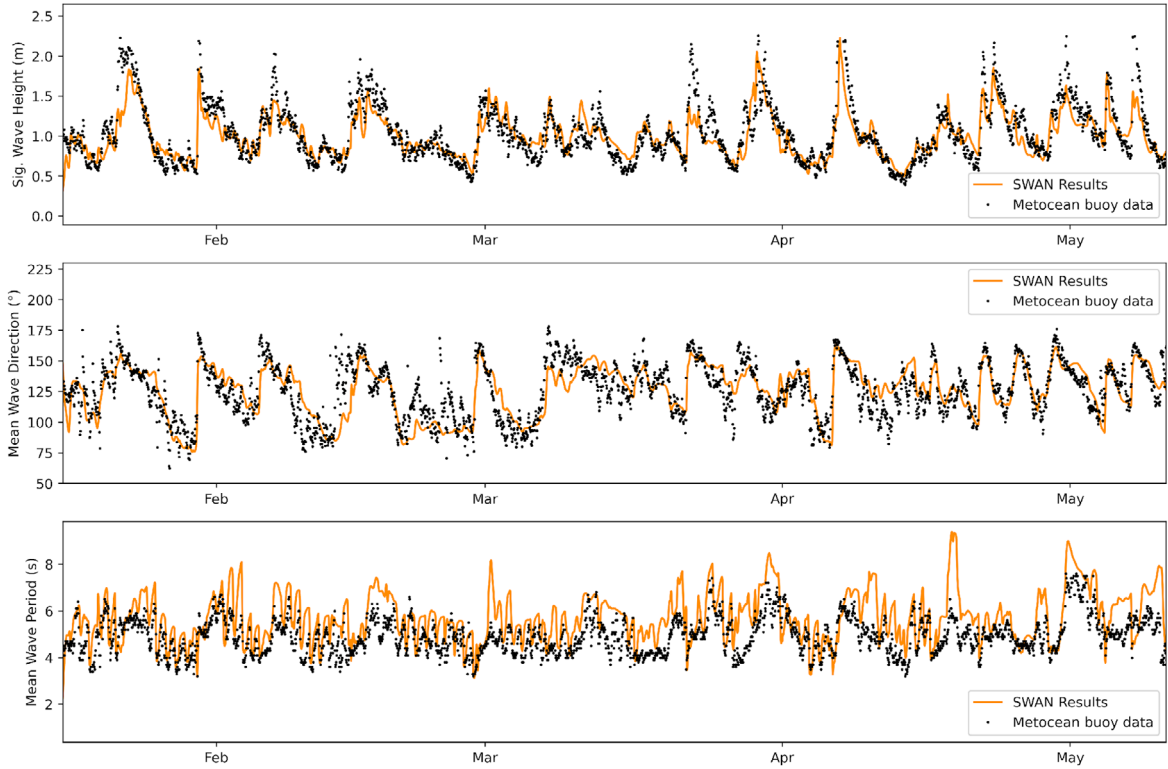


Figure 5. Modeled wave parameters results for significant wave height (H_s), mean wave direction (D_m), mean wave period (T_m), and wave parameters measured by the SiMCosta PR-1 metocean buoy.

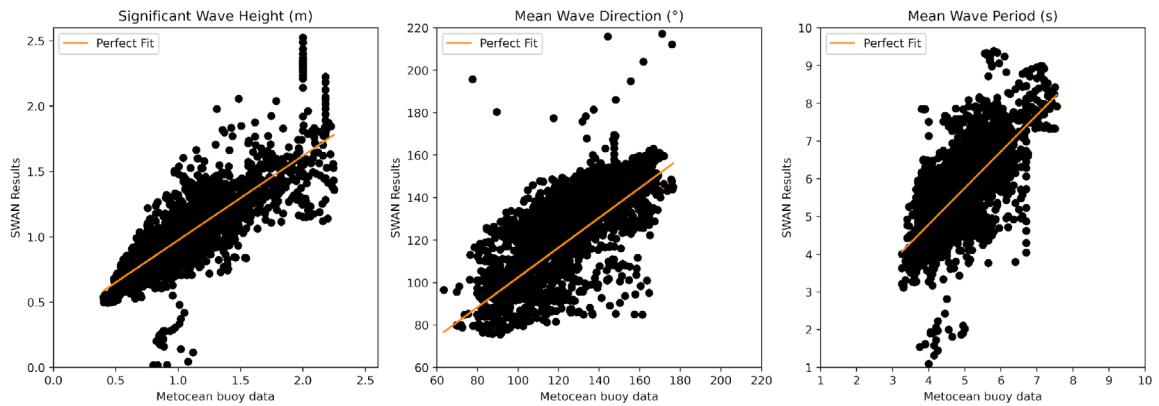


Figure 6. Scatterplots with a perfect fit from the linear regression for significant wave height (H_s), mean wave direction (D_m), and mean wave period (T_m) calculated by SWAN and measured by the SiMCosta PR-1 metocean buoy from January to May 2015.

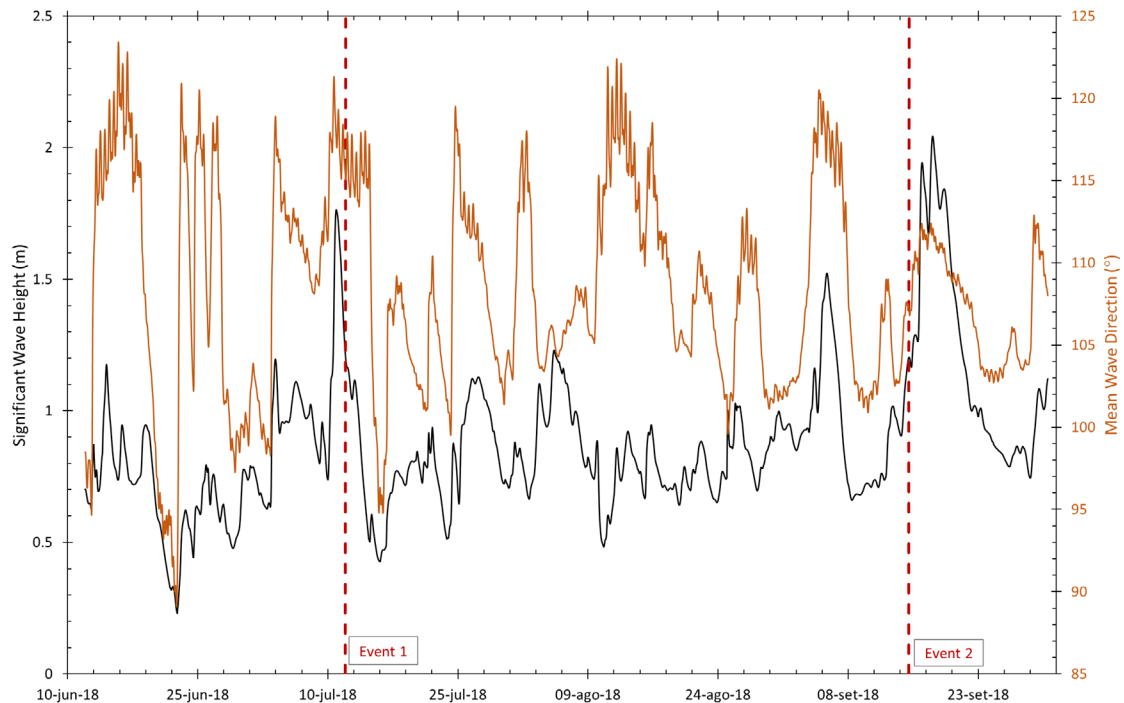


Figure 7. Significant wave height (H_s) and mean wave direction (D_m) during the simulation. Red lines in the plot show two events with the same H_s (1.2 m) but different D_m .

HYDRODYNAMICS AND SEDIMENT TRANSPORT

Figures 8 and 9 show the residual current velocities and bottom sediment transport during the simulation period, from 2018/06/12 to 2018/09/30.

Velocity vectors indicate a residual current direction in the nearshore zone of Matinhos Beach towards the southwest (SW) with magnitudes ranging from 0.15 m s^{-1} to 0.2 m s^{-1} (Figure 8). Nonetheless, in the vicinity of the headland, the generated residual currents pointed to the North-Northeast (N – NE) (Figure 8). The wave rays converge on the headland areas, inducing this phenomenon. The conservation of energy flux results in higher waves on the headland, consequently intensifying the currents to the north and south of the headland. In addition, the energy from waves refracted further north from the headland sustains a recirculation in the nearshore area, possibly triggering the jet stream directed offshore (Figure 8 – zoom). The direction and intensity of the residual sediment transport were similar to the mean currents during the simulation period, with the same convergence

zone near the mouth of the Matinhos River, but without the recirculation in the nearshore area (Figure 9).

The simulation showed significant variations in the littoral drift and nearshore current patterns, as observed in two events during the ebb tide with the same significant wave height ($H_s = 1.2 \text{ m}$), but different incident wave directions in the breaker zone.

During Event 1 (July/12), when the wave direction was 118° , the littoral drift was directed to the N-NE in all domain extensions, showing a continuity in the currents from the headland to the beach (Figure 10). However, during Event 2 (Sept/15), when the wave direction was 107° , the littoral drift pattern was highly similar to the residual current direction for the entire period simulated, with bedload transport to the S-SW (Figures 9 and 11).

The circulation pattern around the headland was also different in each event. The jet stream was stronger and located to the south of the headland in Event 1, with a larger angle of wave incidence (118°). In Event 2, the bedload transport by the jet stream was less intense and closer to the beach to

the north of the headland. The more parallel angle of incidence (107°) in Event 2 favored the formation

of rip currents and a bedload transport divergence zone to the south to the headland. (Figure 11).

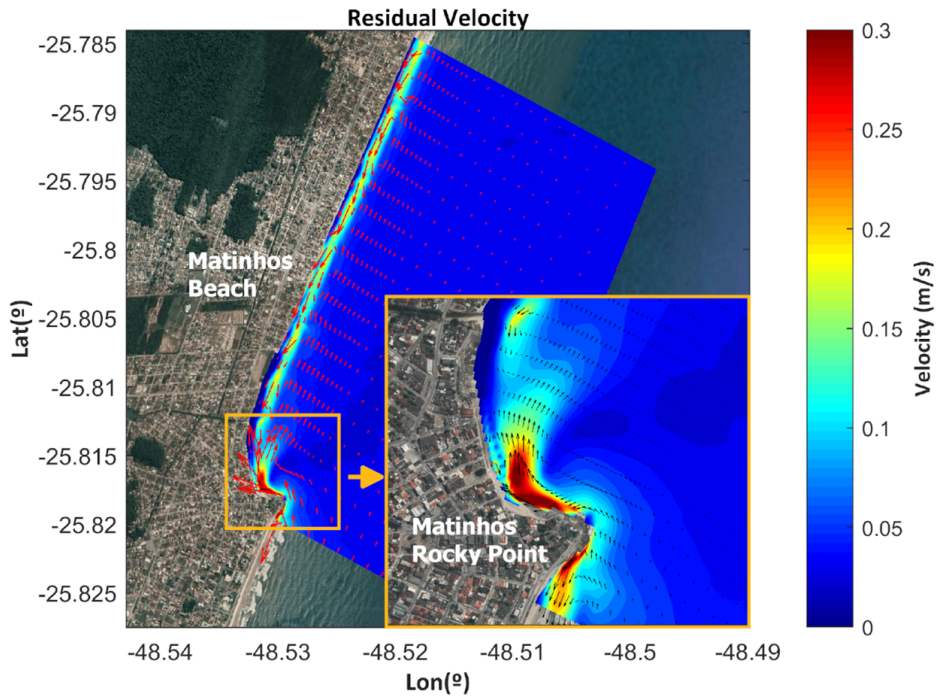


Figure 8. Residual velocity results for Matinhos Beach from 2018/06/12 to 2018/09/30. The yellow square shows a zoomed-in image of the headland.

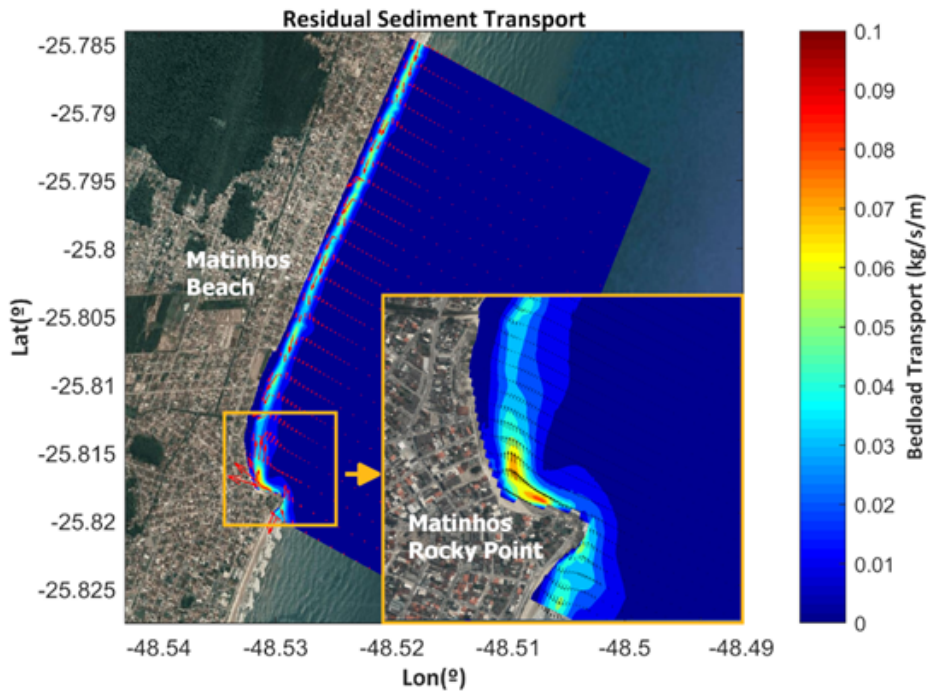


Figure 9. Residual sediment transport for Matinhos Beach from 2018/06/12 to 2018/09/30. The yellow square shows a zoomed-in image of the headland.

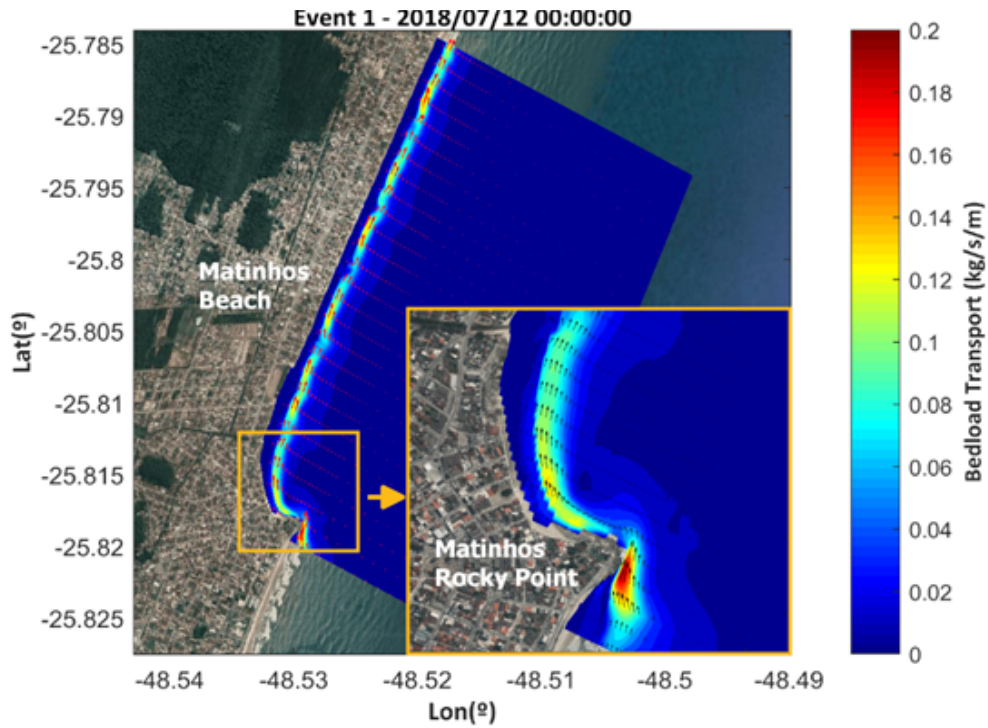


Figure 10. Instantaneous bedload transport pattern for 2018/07/12 00:00h (Event 1) at Matinhos Beach. $H_s=1.2$ m and $D_m=118^{\circ}$ at the offshore boundary. The yellow square shows a zoomed-in image of the headland.

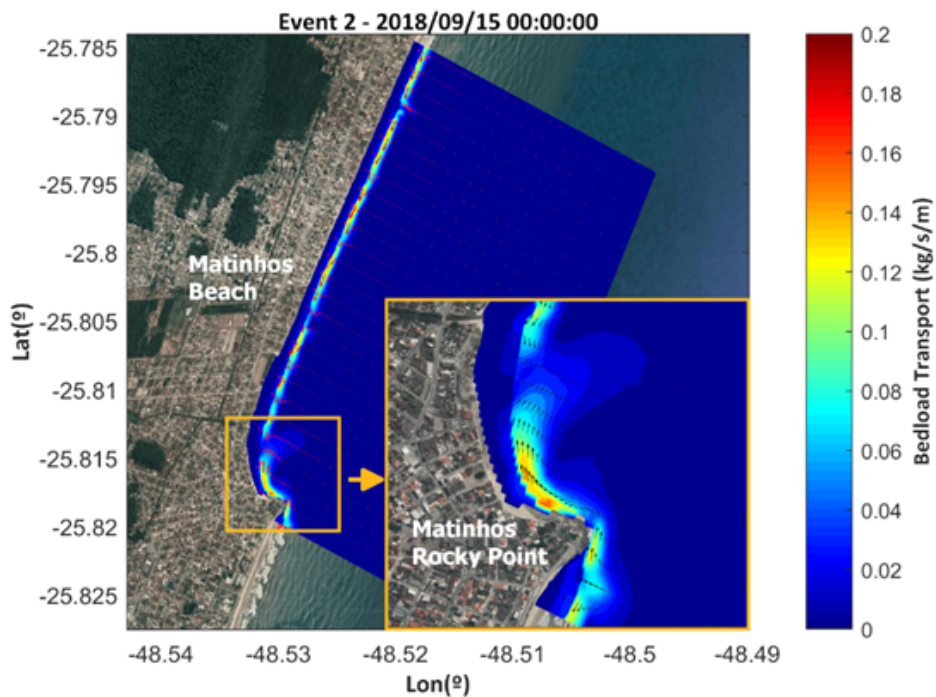


Figure 11. Instantaneous bedload transport pattern for 2018/09/15 00:00h (Event 2) at Matinhos Beach. $H_s=1.2$ m and $D_m=107^{\circ}$ at the offshore boundary. The yellow square shows a zoomed-in image of the headland.

DISCUSSION

Matinhos Beach makes an approximate angle of 24° to the north, which means that waves approaching perpendicular to the coast have an orientation of about 114° . This angle coincides with the predominant direction of the waves in the area (ESE). Because of this, even a slight variation in the angle of wave incidence (10°) can change the direction (southwest or northeast) and intensity of the nearshore current and littoral drift (Figures 10 and 11). For proper prediction and quantification of this process, model uncertainties must be smaller than this slight variation in wave angle. This improved modeling accuracy is only possible with good, detailed bathymetry and time series of wave and current data for validation. However, this does not invalidate the sensitivity of the beach to changes in the direction of the longshore drift with minor variations in the angle of wave incidence.

A possible impact of climate change on the South Brazil Bight is the southward migration of approximately 2° of the South Atlantic Subtropical High center, with potential changes in wind patterns and, consequently, in wave climatology (De Souza et al., 2020). A possible modification in the mean direction of waves may change the dynamic equilibrium of the beach and the erosion/accretion process.

During the winter of 2018, all extreme and destructive events affected the Matinhos coast, which can be observed based on the small morphological changes of erosion in the beach profiles (Figure 3) and the local wave climate (Figure 7). The main morphological change during the surveys was the accumulation of sand in the region adjacent to the headland, represented by Profile I (Figure 3), which rose almost 1 m in height.

The southwestward littoral drift current and the transport convergence near the headland explain the changes (accretion) in Profile I during the study period (Figure 8). This hydrodynamic pattern causes sediment accumulation in the area, enhanced by the secondary circulation caused by the refraction of waves from the headland. The headland acts as a barrier to sediment transported from the northeast. The modeling results confirm the most significant potential for sediment transport near the headland.

On beaches with a log-spiral form, sediment transport along the shore generates erosion or accretion at the ends of the beach (Silvester, 1960). Short-term alterations in shoreline dynamics for such beach types primarily stem from cross-shore transportation processes. Conversely, the long-term transformation is typically linked with longshore drift. Along curved coastlines, the shoreline may gradually pivot around a central point over time in response to shifts in wave directions.

The accretion near the headland and the small morphological changes along Matinhos Beach (Figure 3) corroborate the assumption that the alongshore current was the leading cause of sediment transport during the period. The orientation of the alongshore current suggests that the sediment source is possibly further north from the study area and may be related to the continuous shape of the Matinhos – Pontal do Sul beach arc and the supply of sediment from the Paranaguá Estuarine Complex inlet. The transport of bedload in the southwest-directed nearshore current during one of the most wave-energetic periods of the year (Oliveira et al., 2019) showed a significant fluctuation on a shorter time scale than the predominant littoral drift in the Matinhos – Pontal do Sul beach arc (Bigarella et al., 1978; Angulo, 1992; Noernberg et al., 2007).

The northern sector of the study area (Figure 3) did not show any patterns of erosion or accretion alongshore. However, it is possible to identify that, in general, the accretion zones were located in the upper part of the beach profile and the erosion zones were located in the lower part, next to the waterline. These characteristics are similar to the well-known beach storm profile theory (Komar, 1976), which states that the beach face has an increment in inclination caused by a rise in the energy condition of the system, which is in line with the season in which the study was made.

Recently, sand nourishment was carried out at Matinhos Beach (Ratton, 2020). Nordstrom (2014) suggests that renourishment right in front of a seawall can act as a protection against erosion and restore its recreational benefits, which he claims would probably be effective against the problems previously caused by the construction of a stone seawall at Matinhos Beach, cited by

Angulo et al. (2016), making the beach usable throughout the tidal cycle (Figure 3). However, the comparison between the modeled results (Figure 9) and previous studies on the longshore current in the area shows that variations in its direction can be expected from time to time, which brings considerable uncertainty about the areas where erosion and accretion are expected in response to the construction of groins. Although the coupling of groins and beach nourishment has been successful in some cases (Galgano, 2004; Bocamazo et al., 2011; among others), this uncertainty associated with the direction of the longshore current, if not adequately addressed, can result in a local sediment imbalance, which could even lead to sediment depletion in the area and exacerbate the current problem.

The model implemented in this study can be updated with new bathymetric data and beach profiles and used to help understand and monitor the dynamics of the system under the new conditions, foreseeing the need for possible future interventions.

CONCLUSION

This study assessed the oscillation of the pattern of hydrodynamics and sediment transport in the nearshore zone of Matinhos Rocky Point and Matinhos Beach, showing a transport trend towards the southwest during the winter of 2018. This shows a seasonal variation in the direction of the primary transport trend in the area, which is towards the northeast (Bigarella et al., 1978; Angulo, 1992; Noernberg et al., 2007). This result was achieved by comparing field data and numerical modeling.

Numerical modeling was used to simulate hydrodynamics and sediment transport using the MOHID simulation package. The simulations showed a good agreement between the morphological evolution obtained via field surveys and the transport trend results obtained via numerical modeling. The results reveal that this method may be valuable for understanding the relevant local processes. For this purpose, validating a local morphodynamical model would result in significant knowledge of local sediment dynamics, despite being challenging for the area.

Reliable assessments of shoreline changes are necessary for effective spatial planning, coastal engineering projects, sustainable coastal development, and mitigation of climate change impacts on coastlines. Coastal management plans for the region have been developed, but they sometimes only take into account extreme events and general transport trends over long periods. Based on this study, it became possible to conclude that, for the city of Matinho, it is necessary to consider the wave climate on a seasonal scale, since there is significant sediment transport even in the opposite direction to what would normally be expected. This point may also be valid for other beaches worldwide, which could explain the high number of flawed interventions applied in coastal areas. Another topic highlighted by the study is the need for oceanographic field data for the coastal regions where interventions should be made, because results modeled using global data as input might not be directly addressed, increasing the risk of erroneous conclusions. The unavailability of field oceanographic data is a reality in many countries, especially in developing countries such as Brazil.

This study is intended to expand knowledge of the process in the analyzed region, allowing for different analyses of its characteristics. A sequence with more topographic and bathymetric surveys, an extension of the study area to include the entire Matinhos – Pontal do Sul beach arc, and a more detailed investigation into the sand drift of Caiobá Brava Beach are the keys to improving understanding of the system as a whole. Moreover, some energetic and directional changes are expected to affect the local wave climate in the future, based on its historical trend (Reguero et al., 2013), making the system even more dynamic and bringing more uncertainty to decision-making. The methodology applied can reduce this uncertainty and support effective coastal management.

ACKNOWLEDGMENTS

The authors would like to thank the Coordenação de Aperfeiçoamento de Pessoal de Nível Superior (CAPES, Brazil) for financially

supporting the research project “Desenvolvimento de modelagem oceânica com foco na geração de cenários futuros de mudanças climáticas globais, utilizando o modelo climático global BESM, na plataforma continental e zona costeira do Brasil (ModCosta)” (CAPES: 88887.145863/2017-00) and for granting a MSc scholarship. This study was developed as part of a graduate course on coastal and ocean systems at the Federal University of Paraná (PGSISCO-UFPR). The authors would also like to thank the two anonymous reviewers for their valuable comments on this version of the manuscript. Lastly, the authors thank Prof. Paulo Lana (*in memoriam*) for his immense generosity and contribution as a scientist, teacher, mentor, and friend.

AUTHOR CONTRIBUTIONS

D.M.L.: Conceptualization; Investigation; Formal Analysis; Writing – Original draft; Writing – Review & editing.

A.B.L.; G.A.S.F.: Methodology; Formal Analysis; Writing – Review & editing.

D.M.: Formal Analysis; Writing – Review & editing.

M.A.N.: Conceptualization; Supervision, Investigation; Funding Acquisition; Writing – Review & editing.

REFERENCES

- Alexandrakis, G., Manasakis, C. & Kampanis, N. A. 2015. Valuating the effects of beach erosion to tourism revenue. A management perspective. *Ocean & Coastal Management*, 111, 1–11.
- Angelotti, R. & Noernberg, M. A. 2010. Análise dos riscos ao banho de mar no município de Pontal do Paraná-PR – Temporada 2003/2004. *Brazilian Journal of Aquatic Science and Technology*, 14, 65–75.
- Angulo, R. J. 1992. Geologia da Planície Costeira do Estado do Paraná (Doutorado em Geociências). São Paulo: Universidade Federal de São Paulo.
- Angulo, R. J., Souza, M. C., Muller, E. J., Noernberg, M. A., Oliveira, L. H. S., Soares, C. R., Borzone, C. A., Marone, E. & Quadros, C. L. 2018. Panorama da erosão costeira - Paraná. In: Muehe, D. (Org.). *Panorama da erosão costeira no Brasil* (vol. 1, pp. 586-640). Brasília, DF: MMA.
- Angulo, R. J. 2000. As praias do Paraná: problemas decorrentes de uma ocupação inadequada. *Revista Paranaense de Desenvolvimento*, 99, 97-103.
- Angulo, R. J., Borzone, C. A., Noernberg, M. A., Quadros, J. L., Souza, M. C. & Rosa, L. C. 2016. The State of Paraná Beaches. In: Short, A. D. & Klein, A. H. F. (eds.). *Brazilian Beach Systems*. Cham: Springer International Publishing.
- Bessa Jr, O. 2003. O. Interferência entre a ocupação urbana e a dinâmica natural no Litoral Sul do Paraná. *Análise Conjuntural - IPARDES*, 25(11–12), 13-17.
- Bigarella, J. J., Becker, R.D., Matos, D. J. & Werner, A. 1978. *A Serra do Mar e a porção oriental do estado do Paraná: um problema de segurança ambiental e nacional*. Curitiba: Secretaria de Estado do Planejamento - ADEA (Associação de Defesa e Educação Ambiental).
- Billé, R. 2008. Integrated Coastal Zone Management: four entrenched illusions. *S.A.P.I.E.N.S.*, 1(2). Available from: <https://journals.openedition.org/sapiens/198>. Access date: 05 Jan. 2019.
- Bocamazo, L. M., Grosskopf, W. G. & Buoniato, F. S. 2011. Beach Nourishment, Shoreline Change, and Dune Growth at Westhampton Beach, New York, 1996 – 2009. *Journal of Coastal Research*, 59, 181–191.
- Booij, N., Ris, R. & Holthuijsen, L. H. 1999. A third-generation wave model for coastal regions: 1. Model description and validation. *Journal of Geophysical Research Oceans*, 104, 7649–7666.
- Borzone, C. A., Souza, J. R. B. & Soares, A. G. 1996. Morphodynamic influence on the structure of inter and subtidal macrofaunal communities of subtropical sandy beaches. *Revista Chilena de Historia Natural*, 69, 565–577.
- Cecilio, R. O. & Dillenburg, S. R. 2020. An ocean wind-wave climatology for the Southern Brazilian Shelf. Part I: Problem presentation and model validation. *Dynamics of Atmospheres and Oceans*, 89, 101101.
- Cooper, J. A. G. & Mckenna, J. 2008. Social Justice in coastal erosion management: The temporal and spatial dimensions. *Geoforum*, 39, 294–306.
- De Souza, M. M., Mathis, M., Mayer, B., Noernberg, M. A. & Pohlmann, T. 2020. Possible impacts of anthropogenic climate change to the upwelling in the South Brazil Bight. *Climate Dynamics*, 55, 651–664.
- Ferreira, S.T.A., Amaro, E. V & Santos, T. S. M. 2014. Applied geodesy to integration of topographic and bathymetric data in the characterization of beaches surfaces. *Revista Brasileira de Cartografia*, 66, 167–184.
- Franz, G., Delphey, M. T., Brito, D., Pinto, L., Leitão, P. & Neves, R. 2017a. Modelling of sediment transport and morphological evolution under the combined action of waves and currents. *Ocean Science Discussions*, 13, 673-690. DOI: <https://doi.org/10.5194/os-13-673-2017>
- Franz, G., Leitão, P., Pinto, L., Jauch, E., Fernandes, L. & Neves, R. 2017b. Development and validation of a morphological model for multiple sediment classes. *International Journal of Sediment Research*, 32, 585-596.
- Franz, G., Garcia, C. A. E., Pereira J., Freitas, A. L. P., Rollnic, M., Garbossa, L. H. P., Cunha, L. C., Lentini C. A. D., Nobre, P., Turra, A., Trotte-Duhá, J. R., Cirano, M., Estefen, S. F., Lima, J. A. M., Paiva, A. M., Noernberg, M. A., Tanajura, C. A. S., Moutinho, J. L., Campuzano, F., Pereira, E. S., Lima, A. C., Mendonça, L. F. F., Nocko, H., Machado, L., Alvarenga, J. B. R., Martins, R. P., Böck, C. S., Toste, R., Landau, L., Miranda, T., Santos F., Pellegrini, J., Juliano, M., Neves, R. & Polejack, A. 2021 Coastal Ocean Observing and Modeling Systems in Brazil: Initiatives and Future

- Perspectives. *Frontiers in Marine Science*, 8, 681619. DOI: <https://doi.org/10.3389/fmars.2021.681619>
- Galgano, F. A. Jr. 2004. Long-Term Effectiveness of a Groin and Beach Fill System: A Case Study Using Shoreline Change Maps. *Journal of Coastal Research*, 33, 3-18.
- Griggs, G. B. 2005. The Impacts of Coastal Armoring. *Shore & Beach*, 73, 13-22.
- Hinkel, J., Nicholls, R. J., Tol, R. S. J., Wang, Z. B., Hamilton, J. M., Boot G., Vafeidis, A. T., Mcfadden L., Ganopolski, A. & Klein, R. J. T. 2013. A global analysis of erosion of sandy beaches and sea-level rise: An application of DIVA. *Global and Planetary Change*, 111, 150-158.
- Houston, J. R. 2013. The economic value of beaches - a 2013 update. *Shore & Beach*, 81, 3-10.
- IBGE (Instituto Brasileiro De Geografia E Estatística). 2018. *Modelo de ondulação geoidal*. Rio de Janeiro, IBGE. Available from: <https://www.ibge.gov.br/geociencias/informacoes-sobre-posicionamento-geodesico/servicos-para-posicionamento-geodesico/10855-modelo-de-ondulacao-geoidal.html>. Access date: 17 Sep. 2018.
- IPCC, 2022. *Climate Change 2022: Impacts, Adaptation, and Vulnerability*. Contribution of Working Group II to the Sixth Assessment Report of the Intergovernmental Panel on Climate Change. Cambridge University Press, Cambridge.
- Komar, P. D. 1976. *Beach Processes and Sedimentation*. Hoboken, Prentice Hall.
- Lana, P.C., Marone, E., Lopes, R. M. & Machado, E. C. 2000. The subtropical estuarine complex of Paranaguá Bay, Brazil. In: Seeliger, U., Lacerda L. D. & Kjerfve B. J. (Org.). *Coastal Marine Ecosystems of Latin America* (pp. 131-145). Berlin: Springer Verlag.
- Leitão, P. C. 2003. *Integração de Escalas e Processos na Modelação do Ambiente Marinho* (Ph.D. Thesis). Lisboa: Universidade Técnica de Lisboa.
- Leitão, P. C., Mateus, M., Braunschweig, L., Fernandes, L. & Neves, R. (Ed.). 2008. Modelling coastal systems: the MOHID Water numerical lab. In: Leitão, P. C., Mateus, M., Braunschweig, L., Fernandes, L. & Neves, R. *Perspectives on integrated coastal zone management in South America* (pp. 77-88). Lisboa: IST Press.
- Luijendijk, A., Hagenaars, G., Ranasinghe, R., Baart, F., Donchyts, G. & Aarninkhof, S. 2018. The State of the World's Beaches. *Scientific Reports*, 8, 1-11.
- MARETEC. 2017. *MOHID - Water Modelling System*, Lisboa, MARETEC. Available from: <http://www.mohid.com/>. Access date: 14 Oct. 2017.
- Marone, E. & Camargo, R. 1994. Marés meteorológicas no litoral do Estado do Paraná: o evento de 18 de agosto de 1993. *Nerítica*, 8, 73-85.
- Martins, F. 2000. *Modelação Matemática Tridimensional de escoamentos costeiros e estuarinos usando uma abordagem de coordenada vertical genérica* (Ph.D. Thesis), Lisboa: Universidade Técnica de Lisboa.
- Martins, F., Neves, R. J., Leitão, P. C. & Silva, A. 2001. 3D modelling in the Sado estuary using a new generic coordinate approach. *Oceanologica Acta*, 24, 51-62.
- Marzetti, S., Disegna, M., Koutrakis, E., Sapounidis, A., Marin, V., Martino, S., Roussel, S., Rey-Valette, H. & Paoli, C. 2016. Visitors' awareness of ICZM and WTP for beach preservation in four European Mediterranean regions. *Marine Policy*, 63, 100-108.
- NOAA (National Oceanic and Atmospheric Administration). 2018. *Global Forecast System (GFS)*. Available from: <https://www.ncdc.noaa.gov/data-access/model-data/model-datasets/global-forecast-system-gfs>. Access date: 17 Sep. 2018.
- Noernberg, M., Marone, E. & Angulo, R. 2007. Coastal currents and sediment transport in Paranaguá estuary complex navigation channel. *Boletim Paranaense de Geociências*, 60-61, 45-54.
- Noernberg, M. & Alberti, A., 2014. Oceanographic variability in the inner shelf of Paraná, Brazil: Spring condition. *Revista Brasileira de Geofísica*, 32, 197-206.
- Nordstrom, K. F. 2014. Living with shore protection structures: A review. *Estuarine, Coastal and Shelf Science*, 150 Part-A, 11-23. DOI: <https://doi.org/10.1016/j.ecss.2013.11.003>
- Novak, L. P., Lamour, M. R. & Cattani, P. E. 2016. Vulnerabilidade aos processos erosivos no litoral do Paraná estabelecido pela aplicação da análise multicritérios. *RA'EGA - O Espaço Geográfico em Análise*, 38, 195-218.
- Oliveira, B. A., Sobral, F., Fetter, A. & Mendez, F. J. 2019. A high-resolution wave hindcast off Santa Catarina (Brazil) for identifying wave climate variability. *Regional Studies in Marine Science*, 32, 100834.
- Paraná State Government. 2019. Paraná entrega projeto da orla de Matinhos em Brasília. 2019. *Agência estadual de notícias*, Curitiba. Available from: <http://www.aen.pr.gov.br/modules/noticias/article.php?storyid=102255&tit=Parana-entrega-projeto-da-orla-de-Matinhos-em-Brasilia>. Access date: 30 May 2019.
- Ratton, E. 2020. *Parecer técnico sobre a recuperação da orla de Matinhos, controle de cheias e revitalização urbanística*. Curitiba, UFPR. Available from: <https://itti.org.br/wp-content/uploads/2020/11/parecer-tecnico-recuperacao-da-orla-de-matinhos.pdf>. Access date: 19 Jun. 2023.
- Reguero, B. G., Méndez, F. J. & Losada, I. J. 2013. Variability of multivariate wave climate in Latin America and the Caribbean. *Global and Planetary Change*, 100, 70-84.
- Sampaio, R. 2006. The occupation of Paraná's beach coasts for balneal use. *Desenvolvimento e Meio Ambiente*, 13, 169-186.
- Sayão, O. J. 1989. Littoral drift along some beaches in Brazil. In: Magoon, O. T., Converse, H., Miner, D., Tobin, L. T. & Clark, D. (Ed.). *Proceedings of the 6th symposium on coastal and ocean management* (vol. 4, pp. 3638-3746). Reston: American Society of Civil Engineers.
- Silvester, R. 1960. Stabilization of sedimentary coastlines. *Nature*, 188, 467.
- Souza, M. C., Angulo, R. J., Assine, M. L. & Castro, D. L. 2012. Sequence of facies at a Holocene stormdominated regressive barrier at Praia de Leste, southern Brazil. *Marine Geology*, 291-294, 49-62.

- Soulsby, R. L. & Damgaard, J. S. 2005. Bedload sediment transport in coastal waters. *Coastal Engineering*, 52, 673–689.
- Tolman, H. L., Balasubramanian, B., Burroughs, L. D., Chalikov, D. V., Chao, Y. Y., Chen, H. S. & Gerald, V. M. 2002. Development and implementation of wind generated ocean surface waves models at NCEP. *Weather Forecast*, 17, 311–333.
- Tolman, H. L. 2009. *User Manual and System Documentation of WAVEWATCH III TM Version 3.14*. NOAA/NWS/NCEP/MMAB Technical Note 276. Camp Springs, U. S. Department of Commerce.
- Turki, I., Medina, R., Coco, G. & Gonzalez, M. 2013. An equilibrium model to predict shoreline rotation of pocket beaches. *Marine Geology*, 346, 220–232.
- Umlauf, L., Burchard, H. & Bolding, K. G. O. T. M. 2018. *Sourcecode and Test Case Documentation*. Available from: <http://gotm.net/manual/stable/pdf/a4.pdf>. Access date: 17 Sep. 2018.
- Veiga, F. A. 2004. *Sedimentologia, morfologia & dinâmica da face da costa no litoral central do estado do Paraná*. M.Sc. Geologia Ambiental, Universidade Federal do Paraná.